

## Four-state model of optical collisions: Sr + Ar

J. Light

*Department of Chemistry and James Franck Institute, University of Chicago, Chicago, Illinois 60637  
and Joint Institute for Laboratory Astrophysics, University of Colorado and National Bureau of Standards, Boulder, Colorado 80309*

A. Szöke\*

*Joint Institute for Laboratory Astrophysics, University of Colorado and National Bureau of Standards, Boulder, Colorado 80309*

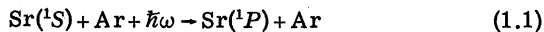
(Received 6 May 1977)

The semiclassical theory of electronic excitation of an atom in a strong nonresonant laser field due to a collision with another atom is presented. It is shown that in the presence of asymptotic degeneracy of the excited state the Landau-Zener two-state model is inaccurate, the exact solution of a two-state model is inaccurate, and both differ qualitatively from the accurate solutions of the equations when all (four) states are included. With parameters chosen to model the process  $\text{Sr}(^1S) + \text{Ar} + \hbar\omega \rightarrow \text{Sr}(^1P) + \text{Ar}$ , cross sections on the order of  $10^{-14} \text{ cm}^2$  are obtained for  $\hbar(\omega - \omega_0) \sim 17 \text{ cm}^{-1}$  over a large range of the Rabi frequency. Depolarization predominates at high field strengths.

### I. INTRODUCTION

In recent years a variety of gas-phase processes occurring in intense laser fields have been studied experimentally and theoretically. These include collisionless multiphoton absorption, collision-induced absorption, and radiative collisions.<sup>1-11</sup> The latter type of processes have been analyzed previously usually in a quasi-two-state approximation in which the collision induces a transition between the two nearly resonant "dressed" states of the atom in the laser field.<sup>3</sup> Due to the dipole selection rules, it is common for either the initial or final states of a dipole-allowed transition to be degenerate, and, due to the collision, one might expect significant coupling between the asymptotically degenerate states.

A preliminary analysis<sup>12</sup> of the experimental results for the process



indicated that a two-state model was not completely consistent with the experimental results. In the two-state model (for appropriate laser intensity and frequency), a single "avoided crossing" of the dressed potential-energy curves appears, with a splitting at the avoided crossing proportional to the field strength. The Landau-Zener (LZ) approximation applied to this situation is accurate only for impact parameters for which the radial turning point is well inside the avoided crossing, i.e., where the avoided crossing is well localized. Since the LZ approximation has been widely used for such processes, we demonstrate explicitly here the hazards associated with such simple models. In addition the two-state model itself, though attractive because of its simplicity, does not contain all the relevant physics of the problem

when more than one upper state interacts.

Consequently, in this paper we investigate the above process in both a two-state and four-state approximation. We present the inadequate two-state model for two reasons. First, the formalism and definitions are simpler to introduce. Second, since it has been the most widely used model for such processes, a demonstration of its inadequacies seems in order.<sup>3,8</sup> In Sec. II, we define the two-state approximation and present the excitation cross sections determined from the LZ approximation, the adiabatic-perturbation approximation, and the numerical solution of the time-dependent Schrödinger equation for this model. We show that even in this case the LZ formula, which is qualitatively correct, may lead to significant numerical errors. In Sec. III the more adequate four-state model is defined and the results of the numerical solution are presented and analyzed in Sec. IV. The results are strikingly different from the two-state model in the high-field region, and the reasons for this are discussed. Finally, in Sec. V the implications of these results are discussed.

### II. TWO-STATE MODEL

In the system (1.1) the  $\text{Sr}(^1P_1)$  is triply degenerate ( $m_j = 0, \pm 1$ ) in the absence of both collisions and the laser field. As a first approximation in a strong linearly polarized nearly resonant laser field one can consider the radiative interaction of the  $\text{Sr}(^1S)$  with the  $\text{Sr}(^1P_1(m_j = 0))$  state only since they are coupled by a dipole-allowed transition matrix element proportional to the field strength. In the absence of collisions, of course, this is a good model of the system. In addition, as will be shown in Sec. III, this would also be a good model

if the  $^1\Sigma$  and  $^1\Pi$  "molecular" interaction potentials between the  $\text{Sr}(^1P_1)$  and  $\text{Ar}(^1S)$  atoms were degenerate at all internuclear separations of importance.

We shall assume the following: (a) A linearly polarized laser radiation field

$$\vec{E} = \hat{e}_z E_0 \cos \omega t.$$

(b) spherically symmetric Van der Waals interaction potentials between the Sr and Ar atoms:  $V_1(R)$  for  $\text{Sr}(^1S) + \text{Ar}(^1S)$  and  $V_2(R)$  for  $\text{Sr}(^1P_1) + \text{Ar}(^1S)$  of the form  $V_i(R) \equiv -C_i^{(i)}/R^6$ . Also we denote  $C \equiv C_6^{(2)} - C_6^{(1)}$ . (c) No coupling terms between the  $\text{Sr}(^1S)$  and  $\text{Sr}(^1P_1^0)$  states due to the Sr-Ar nuclear motion. (d) The transition dipole matrix element is independent of  $R$ ; i.e., the atomic basis is not strongly perturbed by the collision. This approximation is quite good since the transition is allowed. (e) The translational-electronic energy transfer (laser energy defect) is small compared with the average translational energy such that the collision trajectory can be considered to be classical (and, as a further assumption, rectilinear). (f) The laser field is nearly resonant with the atomic transition and the rotating-wave approximation<sup>13</sup> (RWA) is valid. (g) The field ( $E_0$ ) is constant during a collision and the laser frequency,  $\omega$  is far enough off resonance such that one is in the single-collision regime, i.e.,

$$|1/\{\omega - [(\epsilon_2 - \epsilon_1)/\hbar]\}| \ll T,$$

$T$  being the time between collisions.

Given these assumptions we can quantize the  $\text{Sr}(^1P)$  orbitals about the space fixed  $z$  axis, and write the wave function as the linear combination

$$\psi[\chi, R(t), t] = a_1(t)\phi_1(\chi) + a_2(t)\phi_2(\chi), \quad (2.1)$$

where  $R$  is the internuclear separation,  $\chi$  represents the electron coordinates, and the wave functions  $\phi$  are the approximate eigenfunctions of the collisional Hamiltonian

$$\langle \phi_i | \mathcal{H}_0(\chi) + V(\chi, R) | \phi_j \rangle = [\epsilon_i + V_i(R)] \delta_{ij}, \quad (2.2)$$

$$i, j = 1, 2.$$

Asymptotically  $V_i(R \rightarrow \infty) \rightarrow 0$ . The atom-radiation-field matrix elements are

$$\langle \phi_i | \vec{\chi} \cdot \vec{E} | \phi_j \rangle = (\mu E_0 \cos \omega t) \delta_{i, j \pm 1}. \quad (2.3)$$

The matrix representation of the time-dependent Schrödinger equation in this basis is then

$$i \dot{\vec{a}} = \frac{1}{\hbar} \begin{pmatrix} \epsilon_1 + V_1[R(t)] & \mu E_0 \cos \omega t \\ \mu E_0 \cos \omega t & \epsilon_2 + V_2[R(t)] \end{pmatrix} \vec{a} = \vec{W} \vec{a}. \quad (2.4)$$

The assumption (e) of rectilinear trajectories allows  $R$  to be expressed as a function of  $t$ :

$$R^2(t) = b^2 + v^2 t^2, \quad (2.5)$$

where  $b$  is the impact parameter and  $v$  the relative speed of the collision.

We now make a sequence of transformations on Eq. (2.4) to make it more amenable to solution. We shall (see the Appendix for details) (a) make the rotating-wave approximation, (b) remove the trace, and (c) diagonalize asymptotically ( $t \rightarrow \pm\infty$ ).

We then find

$$i \dot{\vec{d}} = \begin{pmatrix} \lambda - \frac{1}{2} V \cos \theta & \frac{1}{2} V \sin \theta \\ \frac{1}{2} V \sin \theta & -\lambda + \frac{1}{2} V \cos \theta \end{pmatrix} \vec{d}, \quad (2.6)$$

where  $\vec{d}$  is related to  $\vec{a}$  by unitary transformations and gives the coefficients of the "dressed" states and with  $\Delta = \omega - (\epsilon_2 - \epsilon_1)/\hbar$  and  $V = (V_2 - V_1)/\hbar$ ,

$$\lambda \equiv \frac{\Delta}{2} \left( 1 + \frac{\mu^2 E_0^2}{\hbar^2 \Delta^2} \right)^{1/2}, \quad \tan \theta \equiv \frac{\mu E_0}{\hbar \Delta}. \quad (2.7)$$

Equation (2.6) is the appropriate equation to solve to determine the time evolution of the dressed-state populations due to a collision. If the field is turned on adiabatically and the Sr atom was initially in the ground state, then the appropriate boundary conditions for (2.6) are  $|d_1(-\infty)|^2 = 1$ ,  $|d_2(-\infty)|^2 = 0$ . Equation (2.6) contains no loss term (imaginary diagonal component for state 2) due to fluorescence since we assume the collision time is much less than the fluorescence lifetime. If the fluorescence is emitted after the collision but during the laser pulse, it will be centered at the ac Stark-shifted frequency

$$\omega_s = -2\lambda + \omega = \frac{E_2 - E_1}{\hbar} \left( 1 + \frac{\mu E_0^2}{\hbar^2 \Delta^2} \right)^{1/2} + \omega \left[ 1 - \left( 1 + \frac{\mu^2 E_0^2}{\hbar^2 \Delta^2} \right)^{1/2} \right].$$

We also note that, as desired, Eq. (2.6) becomes diagonal as  $t \rightarrow \pm\infty$  ( $V \rightarrow 0$ ), and all rapidly varying terms have been eliminated.

Defining the dimensionless quantities

$$\begin{aligned} Z &= \Delta t, \\ R_0^2 &= |C/\hbar\Delta|, \quad \xi = v/\Delta R_0, \\ B &= b/R_0, \\ r^2 &= (R/R_0)^2 = B^2 + \xi^2 Z^2. \end{aligned} \quad (2.8)$$

The problem is parametrized as

$$i \frac{d}{dZ} \vec{d} = \begin{pmatrix} \frac{1}{2\cos\theta} \mp \frac{\cos\theta}{2r^6} & \mp \frac{\sin\theta}{2r^6} \\ \mp \frac{\sin\theta}{2r^6} & -\frac{1}{2\cos\theta} \pm \frac{\cos\theta}{2r^6} \end{pmatrix} \vec{d}, = \underline{W} \vec{d}, \quad (2.9)$$

where the sign depends on the sign of  $C/\Delta$ . We note from Eq. (2.10) that when  $C$  is positive corresponding to a more attractive excited-state interaction and when  $\Delta$  is negative, corresponding to a laser frequency less than the fluorescence frequency, then  $C/\Delta < 0$ , the upper sign is taken in (2.14), and a "crossing point" will occur for impact parameters such that

$$r^6 < \cos^2\theta \text{ or } B^2 < \cos^2/3\theta \text{ (} C/\Delta < 0 \text{)}. \quad (2.10)$$

The problem is now parameterized by three quantities:  $\theta$  (depending on  $E, \Delta$ ),  $B$ , and  $\xi$  (depending on  $v, \Delta$ ).  $R_0$  is a scale factor and does not directly enter Eq. (2.14). This two-state problem may be solved by a number of approximate or exact numerical techniques. The cross sections are defined as

$$\sigma = 4\pi R_0^2 \int_0^\infty B dB P(B). \quad (2.11)$$

In the LZ<sup>14-16</sup> case we have

$$\begin{aligned} P_{LZ}(B) &= 2e^{-\pi^6}(1 - e^{-\pi^6}), \\ \delta &= 0, \quad B^2 > \cos^2/3\theta \\ \delta &= \Lambda B^2 / (\cos^2/3\theta - B^2)^{1/2}, \quad B^2 < \cos^2/3\theta \\ \Lambda &= \tan^2\theta / (12\xi \cos^2/3\theta). \end{aligned} \quad (2.12)$$

The cross section in this case has a maximum for  $\Lambda \approx 0.425$ , and is zero if no curve crossing occurs, i.e.,  $C/\Delta > 0$ .

It was recently shown<sup>17</sup> that adiabatic-perturbation (APT) solutions of equations such as (2.9) are quite accurate over the entire range of parameters, including the case of no curve crossing.

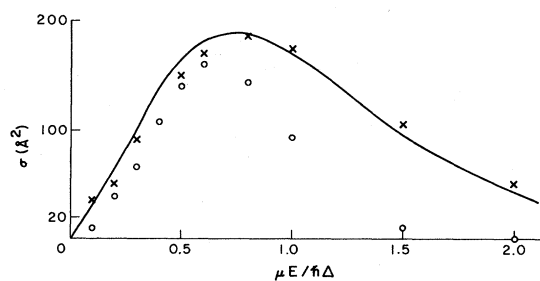


FIG. 1. Cross section for excitation vs  $\mu E/\hbar\Delta$ , curve-crossing case ( $C/\Delta < 0$ ). (—) exact; (××) APT; (○) Landau-Zener.

Again, assuming no phase correlation of the incoming and outgoing trajectories, we have

$$\begin{aligned} \underline{P}_{APT} &= \underline{P}_{APT}(\infty, 0) \underline{P}_{APT}(0, -\infty), \\ \underline{P}_{APT}(a, b) &\equiv \begin{pmatrix} \cos^2 Q(a, b) & \sin^2 Q(a, b) \\ \sin^2 Q(a, b) & \cos^2 Q(a, b) \end{pmatrix}, \end{aligned} \quad (2.13)$$

$$Q(a, b) \equiv \left| \int_a^b dZ \frac{\dot{q}(Z)}{2} \exp \left( -2i \int_a^Z \lambda(Z') dZ' \right) \right|.$$

Thus

$$[P_{APT}(\xi, \theta, B)]_{12} = 2 \sin^2 Q \cos^2 Q = \frac{1}{2} \sin^2(2Q). \quad (2.14)$$

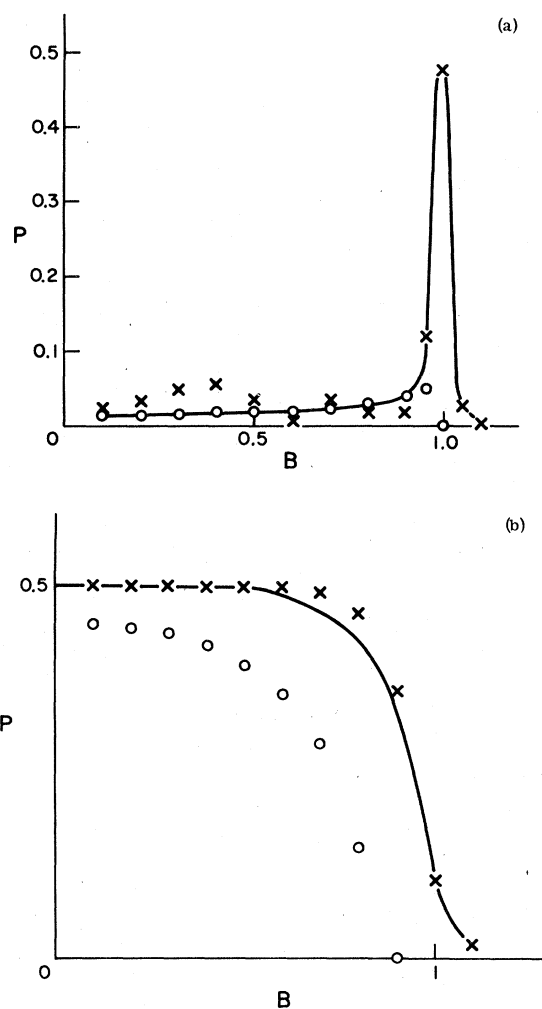


FIG. 2.  $P(b)$  vs  $b$ , two-state model. — exact; (××) adiabatic perturbation approximation; (○) Landau-Zener approximation:  $C/\Delta < 0$ . (a)  $\mu E/\hbar\Delta = 0.1$ ; (b)  $\mu E/\hbar\Delta = 1.0$ .

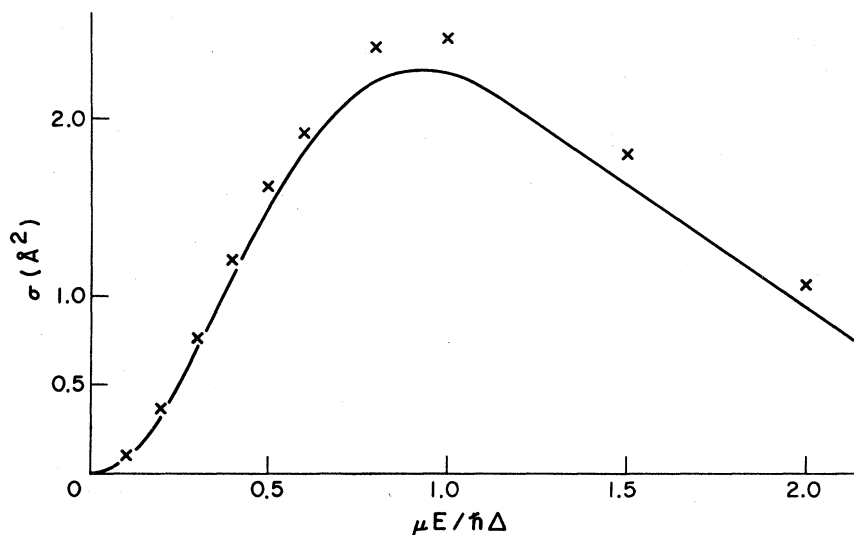


FIG. 3. Cross section for excitation vs  $\mu E/\hbar\Delta$ , no curve crossing ( $C/\Delta > 0$ ). (—) exact; (x) APT.

The integrals were evaluated numerically.

Finally, Eqs. (2.9) were solved numerically by the exponential method,<sup>18,19</sup> again with the assumption of no phase correlation for  $Z \geq 0$ .

The LZ approximation, the APT approximation, and the exact transition probabilities are shown for the case  $\xi = 0.3$  and  $R_0 = 8 \times 10^{-8}$  cm for  $C/\Delta < 0$  (curve crossing) as a function of  $\tan\theta = \mu E_0/\hbar\Delta$  in Fig. 1. Note that the APT result is relatively accurate while the LZ result consistently underestimates the cross section, by a large factor at low and high  $\theta$ . The reason for this is illustrated in Fig. 2 where the transition probability is plotted versus the impact parameter. It is well known<sup>14,15</sup> that the LZ approximation fails for long range (or flat) curve crossings. Thus the LZ result is accurate for small  $B$  where the curves "cross" with significant slope, it underestimates  $P$  for  $B^2 \approx \cos^2/3\theta$  where the curve crossing is disappearing and, of course, gives zero for  $B^2 > \cos^2/3\theta$ . We note, however, that for very low laser intensity, the LZ cross section and that from the exact numerical integration must both go to zero as  $E^2$ .

In Fig. 3 the APT and exact results are given for the case  $C/\Delta > 0$ , with all other parameters as above. Note that the magnitude of the cross section is about  $10^{-2}$  of that in the curve-crossing case (Fig. 1). Thus the model correctly<sup>12</sup> predicts that the cross section for detuning to the red ( $C > 0$ ,  $\Delta < 0$ ) will be much larger than that for detuning to the blue. However, all models predict (for  $C/\Delta < 0$ ) that the cross section should have a relatively sharp maximum for fixed  $\Delta$  as  $E$  is increased. This is not consistent with preliminary experimental results<sup>12</sup> and prompted us to exam-

ine the more realistic four-state model, including the  $m_j$  degeneracy of the  $^1P_1$  state of Sr.

### III. FOUR-STATE MODEL

In this section we take account explicitly of the degenerate nature of the Sr( $^1P_1$ ) upper state for the system (1.1). Although the treatment is specifically for a  $^1S \rightarrow ^1P$  transition, the generalizations to treat other systems are straightforward. We will proceed as follows. In the molecular frame (body fixed) the interaction of the Sr and Ar atoms splits the  $m_j$  degeneracy of the Sr( $^1P_1$ ) states and, in the Born-Oppenheimer approximation, we have only diagonal potential matrix elements in this frame. However, due to the presence of the space-fixed polarized laser field which couples the ground state and the  $m_j = 0$  component of the excited  $^1P_1$  state in the space-fixed frame, it is easiest to transform the molecular Hamiltonian to the space-fixed frame. We then diagonalize the asymptotic Hamiltonian to obtain the atomic "dressed" states and use the RWA to eliminate the time dependence due to the field. Again, assuming a rectilinear trajectory, the time-dependent coupled equations are integrated to obtain the probability matrix for excitation. Integration of the probabilities over the trajectory parameters yields the cross sections.

The Hamiltonian for the system (1.1) is

$$\underline{H} = \underline{H}_{Sr} + \underline{H}_{Ar} + \underline{H}_{coll} + \underline{H}_{field}, \quad (3.1)$$

where the first three terms define the atomic states and the collisional interaction and the last is the interaction with the radiation field. In the

space-fixed atomic basis (for convenience we use the  $x$  and  $y$  basis rather than the  $m_j = \pm 1$  basis)

$$\begin{aligned}\psi_1 &= |\text{Sr}(^1S)\text{Ar}(^1S)\rangle, \\ \psi_2 &= |\text{Sr}(^1P_x)\text{Ar}(^1S)\rangle, \\ \psi_3 &= |\text{Sr}(^1P_y)\text{Ar}(^1S)\rangle, \\ \psi_4 &= |\text{Sr}(^1P_z)\text{Ar}(^1S)\rangle,\end{aligned}\quad (3.2)$$

the matrix representation of

$$\underline{H}_1 = \underline{H}_{\text{Sr}} + \underline{H}_{\text{Ar}} + \underline{H}_{\text{field}} \quad (3.3)$$

is easily evaluated as

$$H_1 = \begin{bmatrix} 0 & 0 & 0 & \mu E_0 \cos \omega t \\ 0 & \hbar \omega_0 & 0 & 0 \\ 0 & 0 & \hbar \omega_0 & 0 \\ \mu E_0 \cos \omega t & 0 & 0 & \hbar \omega_0 \end{bmatrix}, \quad (3.4)$$

where  $\hbar \omega_0 = E(^1P_1) - E(^1S)$  is the energy difference of the Sr excited and ground states,  $\mu$  is the dipole matrix element, and we have chosen the laser polarization along the space-fixed  $z$  axis.  $E_0$  and  $\omega$  are the laser field strength and frequency, respectively.

In the *molecular* frame, with the  $z'$  axis along the internuclear direction, the matrix representation of  $H_{\text{coll}}$  is also diagonal in the molecular rotated basis:

$$\begin{aligned}\psi'_2 &= |\text{Sr}(^1P_{x'})\text{Ar}(^1S)\rangle, \\ \psi'_3 &= |\text{Sr}(^1P_{y'})\text{Ar}(^1S)\rangle, \\ \psi'_4 &= |\text{Sr}(^1P_{z'})\text{Ar}(^1S)\rangle,\end{aligned}\quad (3.5)$$

$$H'_{\text{COLL}} = \begin{bmatrix} V_\sigma & 0 & 0 & 0 \\ 0 & V_\Pi & 0 & 0 \\ 0 & 0 & V_\Pi & 0 \\ 0 & 0 & 0 & V_\Sigma \end{bmatrix}, \quad (3.6)$$

where the diagonal molecular potentials for the upper state are now split into a doubly degenerate  $\Pi$  state and a  $\Sigma$  state.

Again we assume the long-range Van der Waals potentials predominate, and we take

$$V_i = -C_i/R^6. \quad (3.7)$$

For these potentials we take<sup>20</sup>

$$\begin{aligned}C_1 &\ll C_j, \quad j=2,3,4 \\ C_2 &= C_3 = \frac{4}{7}C_4.\end{aligned}\quad (3.8)$$

These are based on the fact that the ground-state interaction potentials should be small, and the

second relation is obtained<sup>20</sup> by assuming the radial portions of the  $\text{Sr}(^1P_1)$  states are not significantly distorted due to the Ar, i.e., no strong chemical binding. This assumption also permits us to use the dipole matrix element associated with the free Sr atom. Equations (3.7) and (3.8), of course, completely neglect the true variation of the potentials for relatively small  $R$ . We do this for two reasons: first, they are unknown and not easily calculated. Although more reasonable guesses than (3.7) could easily be made, the large cross sections found must be dominated by the long-range potentials which are adequately represented by (3.7) and (3.8). In addition, this assumption is consistent with the straight-line trajectories assumed. Thus this model, while simple, should yield the dominant behavior correctly.

Since the matrix representation of the Schrödinger equation must be with respect to a single basis, we will transform the collisional portion of the Hamiltonian from the molecular frame to the space-fixed frame. To do this we operate with the appropriate rotation matrix  $\underline{M}$

$$\underline{H}_{\text{coll}}(\text{space fixed}) = \underline{M}^T \underline{H}'_{\text{coll}} \underline{M}, \quad (3.9)$$

where<sup>21</sup>

$$\underline{M} = \begin{bmatrix} 1 & 0 & 0 & 0 \\ 0 & \cos \theta \cos \phi & \sin \phi \cos \theta & -\sin \theta \\ 0 & -\sin \phi & \cos \phi & 0 \\ 0 & \cos \phi \sin \theta & \sin \phi \sin \theta & \cos \theta \end{bmatrix}, \quad (3.10)$$

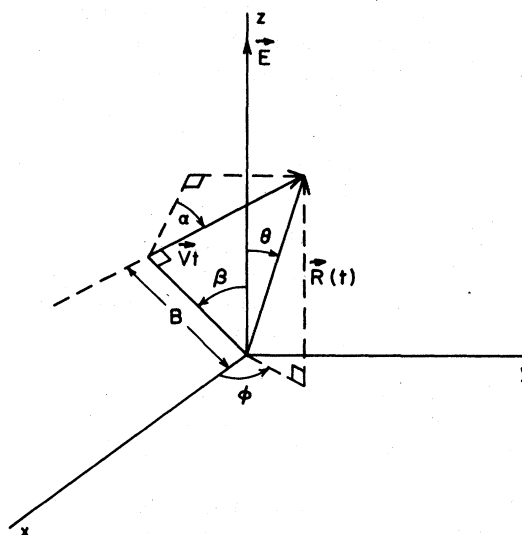


FIG. 4. Geometrical parameters of trajectory (rectilinear).

where we have chosen the  $y'$  axis perpendicular to both  $z$  and  $z'$ .

If the overall wave function is written as

$$\psi = \sum_{i=1}^4 a_i(z) \psi_i, \quad (3.11)$$

the time-dependent Schrödinger equation has the matrix representation

$$i \dot{\vec{a}} = (\underline{H}_1 + \underline{H}_{\text{coll}}) \vec{a}. \quad (3.12)$$

We now make the rotating-wave approximation, diagonalize the asymptotic Hamiltonian to obtain "dressed" states, and remove the trace of the interaction matrix to obtain an equation analogous to (2.9). For the coefficients of the dressed states

$$\frac{T^T \underline{H}_{\text{coll}} T - \frac{1}{4} \text{Tr}(T^T \underline{H}_{\text{coll}} T) I}{4} = \begin{pmatrix} -V_{41} - 2V_{21} \cos q + 4V_{42} \sin^2 \frac{1}{2} q \cos^2 \theta & 2V_{42} \sin \frac{1}{2} q \cos \phi \sin 2\theta & 2V_{42} \sin \frac{1}{2} q \sin \phi \sin 2\theta & (V_{41} - V_{42} \sin^2 \theta) 2 \sin q \\ & V_{21} - V_{42} + 4V_{42} \cos^2 \phi \sin^2 \theta & 2V_{42} \sin 2\phi \sin^2 \theta & 2V_{42} \cos \frac{1}{2} q \cos \phi \sin 2\theta \\ & \text{symmetric} & V_{21} - V_{42} + 4V_{42} \sin^2 \phi \sin^2 \theta & 2V_{42} \cos \frac{1}{2} q \sin \phi \sin 2\theta \\ & & & -V_{41} + 2V_{21} \cos q + 4V_{42} \cos^2 \theta \cos^2 \frac{1}{2} q \end{pmatrix}, \quad (3.15)$$

where

$$\begin{aligned} V_{41} &= -7/4r^6, \quad z = \Delta t, \\ V_{21} &= -1/r^6, \quad \xi = v/R_0 \Delta, \\ V_{42} &= -\frac{3}{4} \frac{1}{r^6}, \quad r^2 = B^2 + \xi^2 z^2, \quad R_0^6 = \left| \frac{(C_2 - C_1)}{\hbar \Delta} \right| \end{aligned}$$

and  $\theta$  and  $\phi$  are the polar angles of the internuclear axis with respect to the space-fixed axis. (We note that since  $H_{\text{coll}}$  commutes with the diagonal matrices used to transform to the rotating-wave representation, it is unchanged by this transformation.)

Equation (3.13) is now in a form amenable to numerical solution. It is asymptotically ( $z \rightarrow \pm\infty$ ) diagonal and the only time- (or  $z$ -) dependent terms are due to the collision. We also note that if the upper  $\Sigma$  and  $\Pi$  states are degenerate,  $V_{42} = 0$ , and the problem becomes block diagonal with only the states 1 and 4 coupled. Thus in this case it reduces exactly to the two-state model considered previously. The time dependence is due to

in terms of the dimensionless variables previously defined:

$$\begin{aligned} \frac{i d \vec{b}}{dZ} &= \mp \lambda \vec{b} + T^T \underline{H}_{\text{coll}} T \vec{b} - \frac{1}{4} \text{Tr}(T^T \underline{H}_{\text{coll}} T) I \vec{b} \\ &= \underline{W} \vec{b}, \end{aligned} \quad (3.13)$$

where the diagonal matrix  $\underline{\lambda}$  has elements

$$\begin{aligned} \lambda_1 &= -\frac{1}{2}(1 + \tan^2 q)^{1/2} - \frac{1}{4} \Delta = -1/2 \cos q - \frac{1}{4} \Delta, \\ \lambda_2 &= \lambda_3 = \frac{1}{4} \Delta, \\ \lambda_4 &= \frac{1}{2}(1 + \tan^2 q)^{1/2} - \frac{1}{4} \Delta = 1/2 \cos q - \frac{1}{4} \Delta, \\ \tan q &= \mu E_0 / \hbar |\Delta|, \end{aligned} \quad (3.14)$$

and the transformed collision matrix is

$\vec{R}(t)$ , the internuclear vector during the collision. The trajectory is specified by the velocity ( $\xi$ ), the impact parameter ( $B$ ), and two angles specifying the direction of the trajectory at the distance of closest approach,  $\alpha$  and  $\beta$ . These angles are shown in Fig. 4. As is apparent from the figure  $0 \leq \beta \leq \pi$ ,  $0 \leq \alpha \leq 2\pi$ , with the weight function  $\sin \beta d\beta d\alpha$ . From the symmetry of the field and time reversal invariance, the probabilities are symmetric about  $\beta = \frac{1}{2}\pi$  and  $\alpha = \frac{1}{2}\pi$  and  $\pi$ . One solves, therefore, for the transition probability matrix for  $Z$  in the range  $(0, -\infty)$  and  $(\infty, 0)$ , then, as before, sets

$$\underline{P}(\alpha, \beta, B, \xi, q) = \underline{P}(\infty, 0) P(0, -\infty). \quad (3.16)$$

Note, however, that although the magnitude  $r(t)$  is symmetric about  $t=0$  (defined as the distance of closest approach), the angles  $\theta$  and  $\phi$  are not. Therefore the equations must be integrated over the entire range of  $z$  for a given trajectory. The cross section is then defined as

$$[\sigma(\xi, q)]_{ij} = R_0^2 \int_0^\infty B dB \left( 8 \int_0^{\pi/2} \sin \beta d\beta \int_0^{\pi/2} d\alpha [P(\alpha, \beta, B, \xi, q)]_{ij} \right). \quad (3.17)$$

Since the cross sections for excitation to each state are obtained, the polarization of the final excitation (or fluorescence) can be obtained. We define the depolarization ratio,  $R$ , in the laboratory frame as

$$R \equiv (\sigma_x + \sigma_y) / \sigma_z. \quad (3.18)$$

#### IV. FOUR-STATE RESULTS

In order to determine the cross sections in Eq. (3.17), the coupled equations (3.14) must be integrated numerically for enough initial values of  $B$ ,  $\alpha$ , and  $\beta$  (for each value of  $\mu E / \hbar \Delta$ ) to evaluate the triple integral in (3.17). This proved to be rather lengthy computationally, requiring about 240 solutions of (3.14) to obtain the cross sections for one value of  $\mu E / \hbar \Delta$  even on what appeared to be a reasonable, if minimal, grid [12 values of  $B$ , 0.2–1.3; 5 values of  $\alpha$  ( $0, \frac{1}{2}\pi$ ) and 5 values of  $\beta$  ( $0, \frac{1}{2}\pi$ )]. Upon investigation, it was determined that the results were not very sensitive to the value of  $\alpha$  (see Fig. 5). The value of  $\alpha = \frac{1}{4}\pi$  only was used subsequently since it preserves the independent and correct average coupling between the  $p_x$  and  $p_y$  orbitals and the initial state. This approximation was checked against the full cross section at  $\mu E / \hbar \Delta = 0.4$ , and agreed reasonably well (<15% deviation of the excitation cross section and <2%

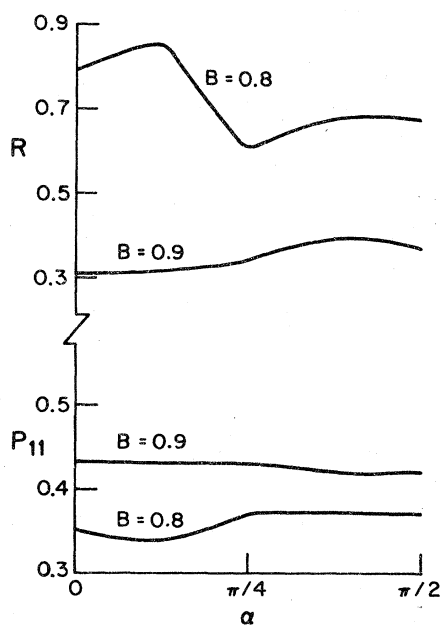


FIG. 5. Variation of  $P_{11}$  and  $R = (P_{22} + P_{33}) / P_{44}$  vs  $\alpha$  for  $B = 0.8, 0.9$ .

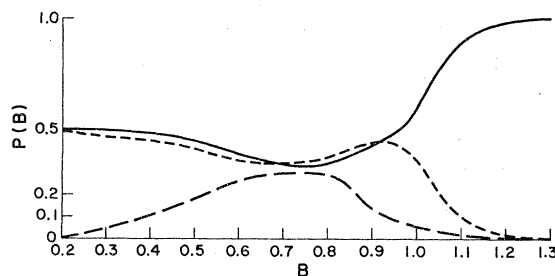


FIG. 6. Probability vs impact parameter, four-state model. (—)  $P_{11}$ ; (---)  $P_{44}$ ; (-\*-)  $P_{22}$ .  $\alpha = 0$ ,  $\beta = \frac{1}{3}\pi$ . (For this  $\alpha$ ,  $P_{33} = 0$ .)

deviation of the polarization ratio). In addition, the integrations for small  $B$  ( $\leq 0.3$ ) took inordinate amounts of time and contributed relatively small amounts to the cross section. Thus trapezoidal-rule integrations over  $B$ ,  $B = 0-1.3$ , was carried out with  $B = 0.5$  the first nonzero point. Checks at one additional value of  $\mu E / \hbar \Delta$  corroborated the above results, and it is conservatively estimated that the results reported are within  $\pm 20\%$  of the exact results for the model. (The model itself is, of course, only a crude but qualitatively correct approximation.)

The values of the parameters used were the following:

$$R_0 = 7.7 \times 10^{-8} \text{ cm}, \quad |\Delta| = 17 \text{ cm}^{-1}, \quad \xi = 0.3. \quad (4.1)$$

These correspond to the parameters used for the two-state model problem, and thus the results can be compared directly.

In Fig. 6 the variation of the excitation-probability matrix elements versus  $B$  are shown. For this relatively weak field strength the excitation is dominated by the  $z$  component. For  $\alpha = 0$  there is (by symmetry) no excitation to the  $y$  component. As in the two-state case the excitation probability falls rapidly for  $B > 1$ . It should be noted that the total probability of excitation in the four-state case can exceed 0.5 in contrast to the two-state model.

In Fig. 7 we plot the total cross section for excitation of the  $\text{Sr}(^1P_1)$  for  $\omega < \omega_0$  (curve-crossing case). For comparison purposes the two-state results are plotted on the same graph. As can easily be seen, the cross sections for small values of  $\mu E / \hbar \Delta$  are very similar, but for values greater than 2, the results are *qualitatively* different, with the excitation cross section remaining high to large field strengths. From Fig. 8, in which the depolarization ratio is plotted one can easily see that this is almost entirely attributable to excitation to the  $P_x$  and  $P_y$  states, with the  $P_z$  excitation

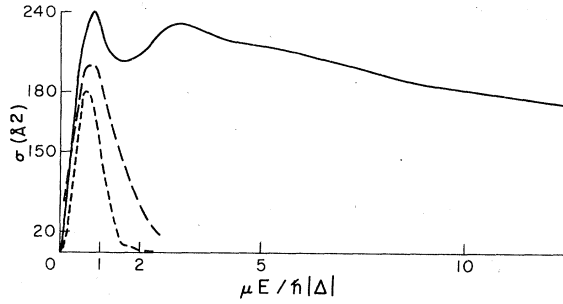


FIG. 7. Total excitation cross section vs  $\mu E/\hbar \Delta$ , four-state model, curve crossings. (—) exact; (—○—○) exact two state; (—·—·) LZ two state.

cross section  $\sigma_{14}$  behaving much like the two-state excitation cross section.

We now look for a qualitative explanation for this behavior. The diagonal elements of Eq. (3.13) as a function of  $r$  for two values of  $\mu E/\hbar \Delta$  are shown in Fig. 9 for  $\theta = \phi = \frac{1}{4}\pi$ . Note that for low-field strength the "crossings" between states 1 and 2 (or 3) and 1 and 4 occur at large values. For high field strengths the ac Stark splitting of the "dressed" states 1 and 4 is so large that the curve crossing occurs at a small value of  $r$ , whereas the Stark-shifted ground state still crosses states 2 and 3 at a relatively large  $r$  value. These changes in crossing points, however, are not in themselves sufficient to cause the very large depolarization ratio found at high-field strengths.

A more plausible explanation lies in the Landau-Zener parameters for each crossing (at fixed

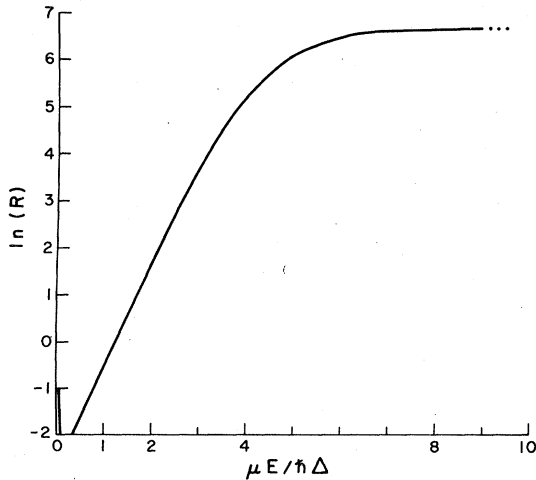


FIG. 8. Depolarization ratio:  $R \equiv (\sigma_x + \sigma_y)/\sigma_z$ .

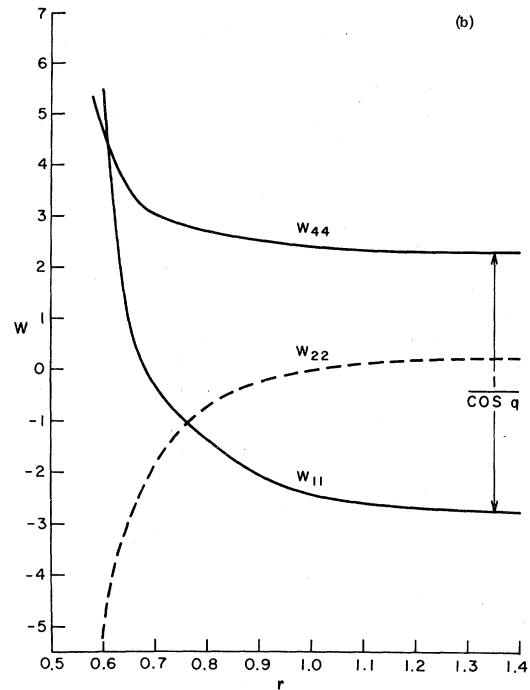
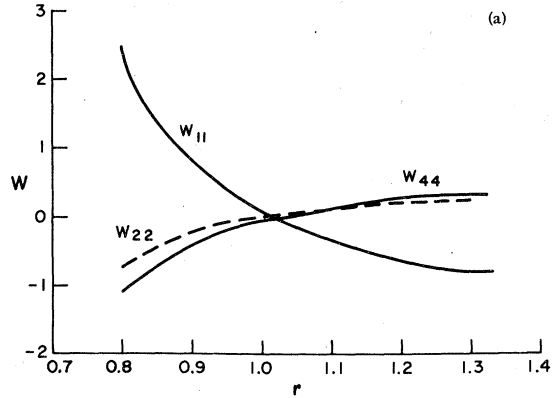


FIG. 9. Diagonal matrix elements of  $W$  vs  $r$ .  $\theta = \phi = \frac{1}{4}\pi$ . (a)  $\mu E/\hbar \Delta = 0.5$  (b)  $\mu E/\hbar \Delta = 5$ .

angle). We define the LZ parameters

$$\delta_{ij} = \left| \frac{2 |W_{ij}|^2}{|d/dz(W_{ii} - W_{jj})|} \right|_{r_{ij}}, \quad (4.2)$$

where  $r_{ij}$  is the crossing point for curves  $i, j$ . For  $\theta = \phi = \frac{1}{4}\pi$  we find, from (3.14 and 3.15)

$$r_{14} = \left(\frac{11}{8} \cos^2 q\right)^{1/6},$$

$$\delta_{14} = \frac{11}{96\xi} \frac{1}{r_{14}^5} \frac{\tan q}{\cos q} \left(1 - \frac{B^2}{r_{14}^2}\right)^{-1/2}, \quad (4.3)$$



TABLE I. Adiabaticity parameters and crossing points  $\xi = 0.3$ ,  $B = 0$ ,  $\theta = \phi = \frac{1}{4}\pi$ .

$\mu E / \hbar \Delta$	$r_{14}$	$\pi \delta_{14}(B=0)$	$r_{12}$	$\pi \delta_{12}(B=0)$
0.5	1.016	0.6195	1.0086	0.00111
1	0.9395	2.318	0.9669	0.0431
5	0.6127	354.4	0.7698	0.5746

and for the 1,2 (or 1,3) crossing

$$r_{12} = \left( \frac{\cos q [1 + (\frac{11}{8}) \cos q]}{(1 + \cos q)} \right)^{1/6}, \quad (4.4)$$

$$\delta_{12} = \frac{3}{64\xi} \frac{\sin^2 \frac{1}{2} q}{[1 + (\frac{11}{8}) \cos q]} \frac{1}{r_{13}^5}$$

$$\times \frac{1}{[1 - (B^2/r_{12}^2)]^{1/2}}.$$

Values of  $r_{ij}$  and  $\pi \delta_{ij}$  are listed in Table I for various values of  $\mu E / \hbar \Delta$  and  $B = 0$ ,  $\xi = 0.3$ . The cross section in a two-state LZ problem has a maximum for  $\pi \delta(B=0) \approx 0.424$ . It is clear that the (1,4) transition becomes quite adiabatic for  $\mu E / \hbar \Delta > 1$ , but the (1,2) and (1,3) transitions do not. Thus for larger values of  $\mu E / \hbar \Delta$  the excitation is primarily to the  $^1P_x$  and  $^1P_y$  states.

When the laser is detuned to the blue, the lower signs in Eq. (3.13) must be used and no curve crossings will occur. In this case, as in the two-state model, the cross sections for excitation are roughly two orders of magnitude smaller ( $\sim 1 \text{ \AA}^2$ ) and are shown in Fig. 10.

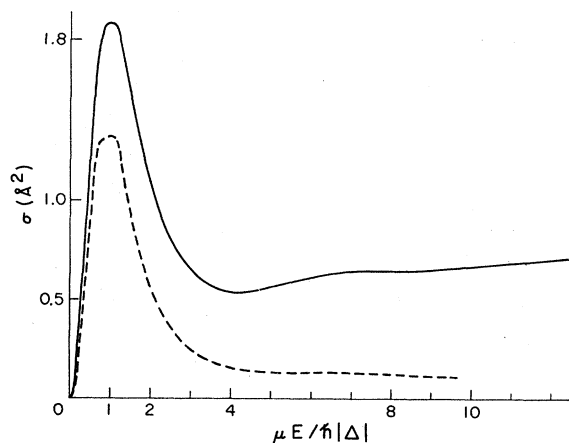


FIG. 10. Excitation cross sections, four-state model, no curve crossings. (—) total excitation; (----)  $\sigma_{44}$ .

## V. DISCUSSION

We have presented calculations for two models of the laser-collision-induced transition (radiative collision) in the  $\text{Sr}(^1S) + \text{Ar} + h\nu$  system. This system has been studied experimentally by Carlsten *et al.*<sup>12</sup> who concluded that the cross section for excitation remained large for large  $\mu E / \hbar \Delta > 2$  when the laser was detuned to the red and that excitation is reduced by about one order of magnitude for equal detuning to the blue.

We have shown that the naive two-state model does not explain the first experimental conclusion and is qualitatively different from the four-state model for which the cross section for excitation remains large for large  $\mu E / \hbar \Delta$ . The qualitative features of the dynamics of the excitation can be understood in terms of the "curve crossings" of the diagonal elements of the effective molecular potentials (rotated to the fixed frame) of the "dressed" states of the atom in the laser field.

Of the assumptions underlying the models, two are seriously open to question. For close collisions ( $R \lesssim 3 \text{ \AA}$ ), the true potentials are clearly going to deviate significantly from the assumed attractive  $R^{-6}$  form. Curve crossings between the upper  $\Sigma$  and  $\Pi$  curves may occur, and both curves will become repulsive for small  $R$ . In addition, for close collisions such as these, the assumed straight-line trajectories will not be correct. For large cross sections (detuning to the red) these two assumptions should be quite good—the most effective impact parameters are 6–9  $\text{\AA}$ . Thus the model should be adequate for this process.

For the laser detuned to the blue, however, there are no long-range curve crossings, the cross sections are small, and the accuracy of the results is more questionable. It is likely in this case that the role of short-range forces will be pronounced, and, in addition, the Boltzmann average over velocities will be important.

Finally, it has been shown that for the curve-crossing case (laser detuned to the red), the proper treatment of the degenerate levels is required to obtain qualitatively correct results, and the use of a two-state model is inadequate. Using the four-state model specific predictions about the polarization of the fluorescence were obtained. It would be interesting to compare them with experiment when data are available.

## ACKNOWLEDGMENTS

The authors would like to thank Chela Kunasz for valuable help in programming these equations and to acknowledge helpful discussions with John Carlsten.

## APPENDIX

The rotating-wave approximation is obtained by transforming (2.4) with a diagonal unitary transformation such that the new off-diagonal elements contain a nonoscillatory portion, and dropping the remaining oscillatory portion.

Let

$$\begin{aligned} \vec{b} &= e^{iqt} \vec{a}, \\ (e^{iqt})_{ij} &= e^{iq_i t} \delta_{ij}, \\ q_1 &= -\frac{1}{2}\omega, \quad q_2 = +\frac{1}{2}\omega. \end{aligned} \quad (\text{A1})$$

Then, in the rotating-wave approximation,

$$\begin{aligned} i\dot{\vec{b}} &= -q\vec{b} + e^{iqt} \vec{W} e^{-iqt} \vec{b} \\ &\approx \begin{pmatrix} \frac{\omega}{2} + \frac{\epsilon_1 + V_1}{\hbar} & \frac{\mu E_0}{2} \\ \frac{\mu E_0}{2} & -\frac{\omega}{2} + \frac{\epsilon_2 + V_2}{\hbar} \end{pmatrix} \vec{b}. \end{aligned} \quad (\text{A2})$$

Removing the trace by the diagonal transformation

$$\begin{aligned} \vec{c} &= e^{i(T_r/2)(t)} \vec{b}, \\ T_r(t) &\equiv \epsilon_1 t + \epsilon_2 t + \int^t (V_1 + V_2) dt, \end{aligned} \quad (\text{A3})$$

we have

$$i\dot{\vec{c}} = \begin{pmatrix} +\eta(t) & \frac{1}{2}\mu E_0 \\ \frac{1}{2}\mu E_0 & -\eta(t) \end{pmatrix} \vec{c}, \quad (\text{A4})$$

where

$$\begin{aligned} \eta(t) &\equiv \frac{1}{2} \left( \omega - \frac{\epsilon_2 - \epsilon_1}{\hbar} - \frac{V_2 - V_1}{\hbar} \right) \\ &= \frac{1}{2} \left( \Delta - \frac{V_2 - V_1}{\hbar} \right) = \frac{1}{2} (\Delta - V). \end{aligned} \quad (\text{A5})$$

Since this representation is not diagonal before and after the collision due to the presence of the laser field, we apply the *time-independent* transformation to the basis of "dressed" states:

$$\vec{d} = \underline{U}_\infty^T \vec{c}, \quad (\text{A6})$$

$$\underline{U}_\infty = \begin{pmatrix} \cos\frac{1}{2}\theta & \sin\frac{1}{2}\theta \\ -\sin\frac{1}{2}\theta & \cos\frac{1}{2}\theta \end{pmatrix}. \quad (\text{A7})$$

The substitution of (A6) into (A4) yields Eq. (2.6).

\*Present address: Lawrence Livermore Laboratory, Livermore, Calif. 94550.

<sup>1</sup>D. A. Copeland and C. L. Tang, *J. Chem. Phys.* **65**, 3161 (1976).

<sup>2</sup>L. I. Gudzenko and S. I. Yakovlenko, *Zh. Eksp. Teor. Fiz.* **62**, 1686 [*Sov. Phys. JETP* **35**, 877 (1972)].

<sup>3</sup>N. M. Kroll and K. M. Watson, *Phys. Rev. A* **13**, 1018 (1976).

<sup>4</sup>A. M. F. Lau, *Phys. Rev. A* **13**, 139 (1976).

<sup>5</sup>J. I. Gersten and M. H. Mittleman, *J. Phys. B* **9**, 383 (1976).

<sup>6</sup>J. M. Yuan, T. F. George, and F. J. McLafferty, *Chem. Phys. Lett.* **40**, 163 (1976).

<sup>7</sup>J. C. Y. Chen, T. Ishihara, and K. M. Watson, *Phys. Rev. Lett.* **35**, 1574 (1975).

<sup>8</sup>V. S. Lisitsa and S. I. Yakovlenko, *Sov. Phys. JETP* **41**, 233 (1975); **39**, 759 (1974).

<sup>9</sup>S. Geltman, *J. Phys. B* **9**, L569 (1976).

<sup>10</sup>J. M. Yuan, J. R. Laing, and T. F. George, *J. Chem. Phys.* **66**, 1107 (1977).

<sup>11</sup>E. Courtens and A. Szöke, *Phys. Rev. A* **15**, 1588 (1977).

<sup>12</sup>J. Carlsten, A. Szöke and M. G. Raymer, *Phys. Rev. A* **15**, 1029 (1977); A. Szöke, *Opt. Lett.* **2**, 36 (1978).

<sup>13</sup>A. Abragam, *Principles of Nuclear Magnetic Resonance* (Clarendon, Oxford, 1961).

<sup>14</sup>J. B. Delos and W. R. Thorson, *Phys. Rev. A* **6**, 728 (1972); see also M. B. Faist and R. D. Levine, *J. Chem. Phys.* **64**, 2953 (1976); M. B. Faist and R. B. Bernstein, *ibid.* **64**, 2971 (1976).

<sup>15</sup>G. A. L. Delvigne and J. Los, *Physica (Utr.)* **67**, 166 (1973); D. R. Bates, *Proc. R. Soc. Lond. A* **257**, 22 (1960).

<sup>16</sup>L. D. Landau, *Phys. Z. Sov.* **2**, 46 (1932); C. Zener, *Proc. R. Soc. Lond. A* **137**, 696 (1932).

<sup>17</sup>J. C. Light, *J. Chem. Phys.* **66**, 5241 (1977).

<sup>18</sup>P. Pechukas and J. C. Light, *J. Chem. Phys.* **44**, 3897 (1966).

<sup>19</sup>J. C. Light, in *Methods in Computational Physics*, edited by M. Rotenberg (Academic, New York, 1971), Vol. 10.

<sup>20</sup>A. Gallagher and T. Holstein, *Phys. Rev. A* **16**, 2413 (1977).

<sup>21</sup>M. Rose, *Elementary Theory of Angular Momentum* (Wiley, New York, 1957).